Pis'ma v ZhETF, vol. 83, iss. 5, pp. 246 – 250 © 2006 March 10

Ion acceleration at the front and rear surfaces of thin foils with high intensity 40 fs laser pulses

S. Ter-Avetisyan[1)], *P. V. Nickles*

Max-Born-Institute, D-12489 Berlin, Germany

Submitted 23 January 2006

Ion acceleration from the front and rear sides of a foil target is observed by measurements of the ions' spectral and spatial emission characteristics when irradiating the targets with ultra-short (40 fs) high-intensity laser pulses. The experimental results show that the origin of accelerated ions, both from the front and rear surfaces of the target, strongly depend on the laser energy absorption mechanism. In particular, laser pulse parameters, such as pulse duration and contrast, are crucial and determine the entire acceleration scenario. Thus the experimental outcome can be controlled by selection of the irradiation conditions.

PACS: 41.75.Jv, 52.38.Kd, 52.50.Im

Recent high intensity laser-plasma interaction experiments have shown unique features such as the acceleration of electrons to energies more of than 100 MeV, of ions to a few tens of MeV, and many other phenomena (e.g. see [1]). For the present case, ion generation beam-like characteristics such as high collimation, high particle flux and short pulse duration have been demonstrated, which make them attractive for new applications. However, in spite of extensive studies, the origin and the mechanism of ion acceleration are still a matter of discussion. Ions are created and accelerated either at the rear surface [2 – 4] through the self-consistent electrostatic accelerating field generated by fast electrons escaping in vacuum (the so-called Target Normal Sheath Acceleration – TNSA mechanism) or at the target front surface, illuminated by the laser [5 – 7]. Particle-in-cell (PIC) simulations suggest a variety of mechanisms that may be responsible for acceleration at the front surface: formation of multiple collisionless electrostatic shocks at high plasma density [8 – 10]; a solitary wave produced by shock-wave decayin a plasma slab [11] irradiated by an intense picosecond laser pulse; or a mechanism wherein the short laser pulse ponderomotive pressure displaces the background electrons, and the ions are accelerated by the electrostatic field of the propagating double layer [12] thus formed.

Up to now, it is not clear which process; rear or front surface acceleration is dominant. Since unambiguous experimental observations by different groups were explained invoking different acceleration scenarios, it is likely that specific experimental conditions used in different experiments, such as laser pulse duration, pulse shape/contrast, or target properties play a fundamental role. PIC simulations [13, 14] and the observations in [15, 16] show that ions can be produced at the front and the rear sides simultaneously, even if the generation processes are quite different.

In this letter we discuss peculiarities of the ion acceleration from the rear and front sides of thin foil targets, irradiated by ultrashort (sub 50 fs) high intensity ($\sim 10^{19}$ W/cm^2) laser pulses, via space charge displacement due to resonance absorption and the action of the laser ponderomotive force on the electrons. The investigations showed that the laser pulse contrast plays a fundamental role for the interaction. This is, to our knowledge, the first observation of the ions accelerated from the front and the back sides of the thin foil target exhibiting distinct differences in their origins and in the phenomena responsible for different acceleration scenarios. Previously it was shown that the duration of the laser prepulse has a profound effect on the maximum proton energy [17]. Now, we show directly that the entire ion acceleration scenario can be controlled. A simple geometry of laser-target interaction is used to elucidate the particle acceleration dynamics.

The absorption mechanisms of intense laser radiation at the target are the basic processes in laser-matter interaction studies. Inverse bremsstrahlung and resonance absorption are very familiar. Whereas inverse bremsstrahlung has a maximum absorption accompanied by efficient generation of a hot electron population when the irradiation is normal to the target plane, resonance absorption can drive efficiently electrons to high energies at non-normal angles of laser incidence. These electrons create a smooth density and temperature profile in the interior region of the target, with a maximum in a direction normal to the target. The electrostatic sheath thus built up accelerates the ions. The conver-

[1)] e-mail: sargis@mbi-berlin.de

sion of the incident radiation energy to the plasma could be as high as 50%.

At high-intensity laser irradiation, the ponderomotive force [18 – 20] also starts to play a decisive role. In contrast to inverse bremsstrahlung and resonance absorption, which causes the quiver motion of the electrons in the oscillating field of the laser, the ponderomotive force accelerates the electrons in the laser propagation direction if the laser intensity gradient is high enough; e.g. if the laser pulse length is shorter than its focal spot diameter. The ponderomotive force drives the electrons with a step- or plateau-like density profile, and has a strong directionality along the laser propagation direction. The laser energy transfer to the hot electrons could also be carried by fast plasma waves through the nonlinear ponderomotive force [21] and by the laser field itself [22]. These mechanisms are not mutually exclusive. Their relative contributions depend strongly upon the particular target and laser parameters, and could give a contribution to the generation of electrons and, in turn, to ion acceleration mechanisms.

In the experiment [23], irradiating planar targets at angles less than 45° to the normal with intense 100 fs laser pulses, it was shown that indeed two groups of separately located hot electron populations were present at the target rear side. The authors attribute that to the electrons resulting from resonance absorption (e_R^- in Fig.1) propagating in the target normal direction whereas, the ponderomotively-accelerated electrons (e_p^- in Fig.1) propagate in the laser irradiation direction. In terms of ion acceleration, it is obvious that both electron populations at the target rear side would create electrostatic fields that accelerate ions/protons according to the TNSA mechanism. This means that, at the target rear surface, one also has two sources from which the ions are accelerated (Fig.1). The acceleration direction of ions from the rear side is always normal to the target, while ions from the front side of the target could be accelerated also in the direction of the ponderomotively driven electrons. Those ions propagate through the target, leaving the target rear surface in the laser propagation direction. Therefore, one can expect ion emission in two directions: either in the laser propagation direction due to ponderomotively driven electrons, or normal to the surface due to electrons driven by resonance absorption, depending on which laser energy absorption mechanism is dominant. If both mechanisms are equivalent, then one could observe widely spread proton emission as described in [24]. Therefore, measuring the angle-resolved ion emission as well as spatially-resolved ion source characteristics under conditions where the laser energy absorption mechanisms are well-defined, one could clarify whether

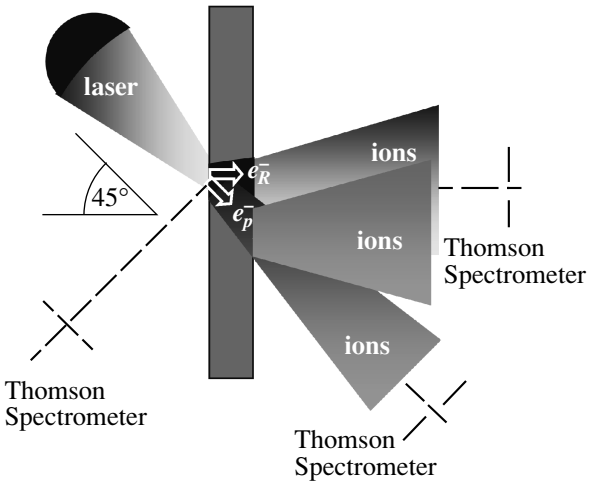

Fig.1. Schematic of the experiment showing two ion beams accelerated due to the hot electron populations created by resonance absorption (e_R^-) and ponderomotive acceleration (e_p^-) directed normal to the target surface and in the laser irradiation direction, respectively. Both electron populations at the target rear side would create electrostatic fields separated in space that could accelerate the ions. The ions from the rear side will be accelerated in the direction of the target normal, whereas the ions from the front side are accelerated not only in the target normal direction due to (e_R^-) electrons, but also they could be accelerated in the direction of the ponderomotive electrons (e_p^-); that is, in the direction of laser propagation

the ions come from the front or rear surface of the target.

In our experiments, thin (20 μm) planar Mylar foil targets were irradiated by $\leq$ 50 fs, 700 mJ Ti:Sapphire laser pulses [25]. With an f/2.5 off-axis parabolic mirror, a maximum vacuum intensity of $1.2 \cdot 10^{19}$ W/cm^2 was reached. The temporal contrast of the laser pulse was characterized by a scanning third order cross correlator with a dynamic range of 10^{10}, having a temporal resolution of 150 fs and a scanning range of $\pm$200 ps. The pulse shape several ns before main pulse was controlled by fast photodiode with temporal resolution about 300 ps. In typical operation conditions the amplified spontaneous emission (ASE) pedestal of the laser pulse in a temporal window of several picoseconds before the pulse peak had a relative value of about $5 \cdot 10^{-7}$. The ASE pedestal could be reduced by driving the three amplifiers of the Ti:Sapphire laser with specifically delayed pump mode. This led to a reduction of output pulse energy up to 550 mJ, but to an improvement of the ASE level down to 10^{-8}. The pulse shape close to the peak was unchanged, and in both cases no pre-pulses preceding the main pulse were observed.

Measurements of the ion energies were carried out with a Thomson parabola spectrometer, where the ions were detected by an absolutely calibrated 40 mm multichannel plate (MCP) coupled to a phosphor screen [26] enabled for single-particle detection. (For further details, see in [27].) It should be noticed that background pressure in the experimental chamber was a few times 10^{-6} mbar, and in the spectrometer even lower. For the spatially resolved measurements, three Thomson spectrometers with an acceptance angle of 256 nsr were positioned around the target at 0, 45, and 135° from the laser propagation direction (Fig.1). Spatial and energy distributions of the ions were measured for normal and 45° laser irradiance of the target.

At normal laser incidence on the target and with an improved laser pulse contrast of up to 10^{-8}, an ion spectrum was registered only in the target normal direction (Fig.2). Ions were emitted neither at 45° (in contrast

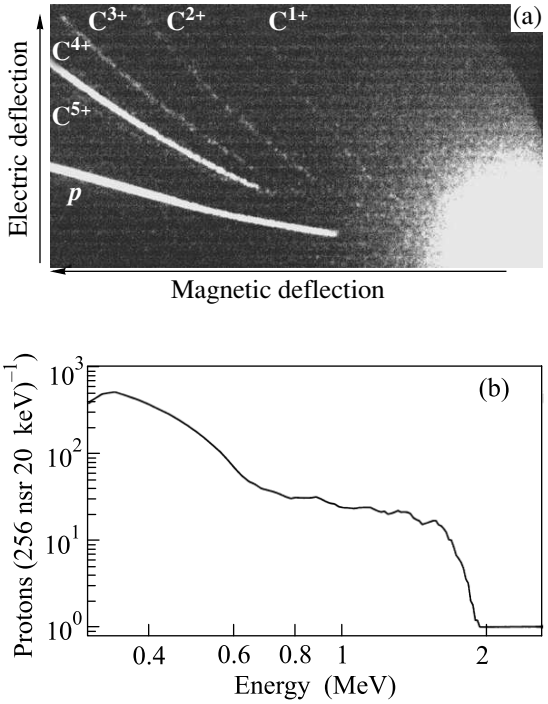

Fig.2. (a) The CCD picture from the MCP-phosphorous screen of an ion spectrum measured in the direction of the target normal. Here C^{1+}, C^{2+}, C^{3+}, C^{4+}, and a weak signal from C^{5+} ions, as well as a proton signal could be identified. (b) The proton spectrum deduced from this digital image at normal laser incidence on the target

to [24]) nor at 135° to the target normal. In this interaction geometry it is obvious that the hot electrons, no matter how they are created, will build up the acceleration field which in turn accelerates the ions either from the front or rear side of the target only in a direction

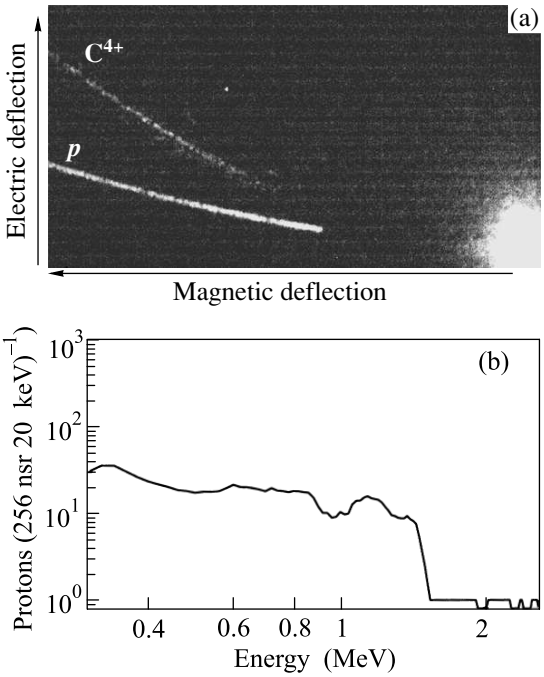

Fig.3. (a) The CCD picture of accelerated ion spectra; (b) deduced proton spectra at 45° laser incidence on the target measured in the direction of laser propagation. Here C^{4+} ions and the proton signal could be identified. There is no signal from low charge states of carbon ions

normal to the target. This result is in agreement with [5] and many others, which have reported ion emission at an angle within 15–20°. Fig.2 depicts a) an ion spectrum image from the MCP-phosphorous screen, and b) a proton spectrum deduced from this digital image. In Fig.2a one can identify protons, carbon ions from C^{1+} up to C^{4+}, and weak C^{5+} ion signals. An intrinsic feature of Fig.2a is the pronounced C^{4+} ion emission.

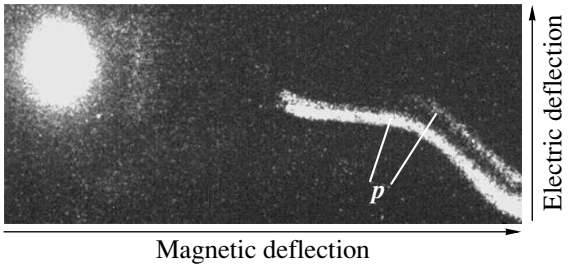

Fig.4. The CCD picture of the proton spectrum at 45° laser incidence on the target measured in the direction of the target normal. Two parallel proton parabolas show the existence of the two sources of emission

When the target was turned to 45° with respect to the laser incidence, and all other experimental conditions were kept constant, we measured in the direction of laser

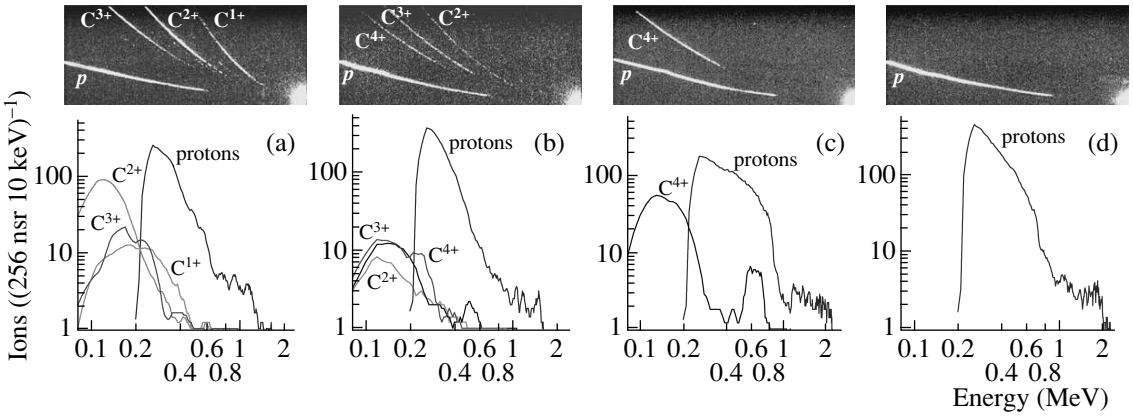

Fig.5. At a laser pulse contrast level of $5 \cdot 10^{-7}$, the emitted ion spectra are shown as measured in the direction of the target normal at 45° laser incidence on the target for 4 successively increasing laser intensities: (a) $2 \cdot 10^{18}$ W/cm^2; (b) $3 \cdot 10^{18}$ W/cm^2; (c) $5 \cdot 10^{18}$ W/cm^2; (d) $10 \cdot 10^{18}$ W/cm^2. On the top are depicted the CCD pictures of the ion spectra, and the corresponding evaluated spectra are shown on the bottom

propagation only protons and C^{4+} ions (Fig.3). The ions emitted in the laser propagation direction should stem only from the front surface (Fig.1), accelerated by a field built up due to the ponderomotively driven electron population from the front surface. Additionally, according to our supposition above, one could also expect two ion sources at the rear side of the target emitting ions normal to the target (Fig.1). In order to prove that, we performed an energy-dispersed pinhole imaging of the source. The source at the target rear surface was imaged with high magnification on an MCP detector plate by placing the entrance pinhole of the Thomson spectrometer (with a diameter of 30 μm) at a distance of 5 cm from the source. This made it possible to image the ion source with a 15 times magnification, and simultaneously to record the ion energy distribution. (For further details, see [28]). The two parallel proton traces measured in the direction normal to the target surface (Fig.4) are indicative of two separate proton sources. The second source (or second proton trace) appeared only when protons were measured in the laser propagation direction. It is worth noting that C^{4+}ions measured in the laser direction are of the highest charge state that can be easily ionised by above threshold ionisation [29] at the laser intensities used, and which could then undergo an acceleration process. This is in good agreement with a model calculation given in [4], that all carbon ions are sequentially ionised up to C^{4+}. This picture is a particular characteristic of a plasma created by highly contrasted laser pulses. Additionally, the protons from the front side have a plateau-like spectrum with a sharp cut off (Fig.3). This is consistent with predictions of PIC simulations [9, 10] that the interaction of collisionless electrostatic shocks formed at the front surface are responsible for the observed plateau structure in the ion spectrum, and that the plateau provides a direct signature for shock acceleration at the front surface of the target.

In contrast to that, at the same interaction geometry with a target at 45° but at a reduced laser pulse contrast to a "typical" level of $5 \cdot 10^{-7}$, no ions were registered in the laser direction and no second ion source at the target rear side was observed. Fig.5 shows the emitted ion spectra in the direction normal to the target at four successively increasing laser intensities (from (a) to (c)). No pronounced emission in any of the ion species could be recorded. This is consistent with a picture of the interaction such that the laser energy absorption is dominated by resonance absorption, and the created smooth electron density and temperature profiles in the interior region of the target would ionise and accelerate the ions in the direction of the target normal. The correlation between the laser intensity and proton cut-off energy with the ion charge states is clearly visible. From Fig.5, the total ion yield, and the yields of protons and carbon ions, have a dependence on laser pulse intensity as depicted in Fig.6. With an increase in the laser intensity, the total ion yield increases, but only due to an increase of the proton yield because the carbon ion yield decreases. Additionally, an increase of laser pulse intensity (Fig.5) is accompanied by growth of the ion charge states. Finally, when the laser intensity is about 10^{19}W/cm^2, only protons are detected and no more carbon ions could be recorded (Fig.5d). These observations show that if the high acceleration field is build up rapidly due to a short laser pulse, the protons as the lightest ions are accelerated first, and they could consume all the energy of

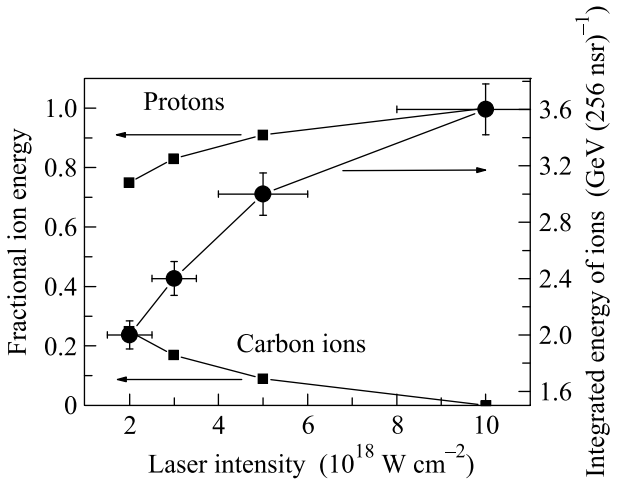

Fig.6. The total ion yield, and the proton and carbon ion yields as a function of laser pulse intensity are shown, as deduced from Fig.5

the accelerating field, since the number of protons is not limited under our conditions. It is worth noticing that no ion emission was observed at 135° in any case. Additionally, in contrast to the protons from the front side, which have a plateau-like spectrum with a sharp cut off energy (Fig.3), the proton spectrum from the rear side (Fig.5) shows a rapidly decreasing distribution.

To summarise, we have measured protons and ions accelerated from the front and rear side of a thin Mylar target irradiated by ultrashort (40 fs) and high intensity ($1.2 \cdot 10^{19}$ W/cm^2) laser pulses. This is, to our knowledge, the first observation of particle acceleration from the front and rear sides of the target, exhibiting distinct differences depending on their origin and on the phenomena responsible for the different acceleration scenarios. High laser pulse contrast can cause directed ion acceleration from the front surface of the target, while a relatively low contrast accelerates the ions only from the rear surface. For efficient acceleration of ions to high energies, laser pulses with a very high contrast should be applied to the thin foil target in order to have direct ion acceleration from the front surface and reduced electron and ion energy losses in the target material. Additionally, because here the electrons are driven ponderomotively during the laser pulse, it is thought that they could accelerate bunches of protons from the front side of the target with very short pulse duration, which is not the case for ions from rear side. We have shown that the ion acceleration scenario can be controlled by laser pulse contrast variation.

We acknowledge stimulating discussions with M. Schnürer and H. Reiss. This work was partly supported by DFG-Project SFB-Transregio TR 18.

1. D. Umstadter, J. Phys. D: Appl. Phys. **36**, R151 (2003).
2. R. Snavely, M. H. Key, S. P. Hatchett et al., Phys. Rev. Lett. **85**, 2945 (2000).
3. A. J. Mackinnon, M. Borghesi, S. Hatchett et al., Phys. Rev. Lett. **86**, 1769 (2001).
4. M. Hegelich, S. Karsch, G. Pretzler et al., Phys. Rev. Lett. **89**, 085002 (2002).
5. E. L. Clark, K. Krushelnick, J. R. Davies et al., Phys. Rev. Lett. **84**, 670 (2000).
6. A. Maksimchuk, S. Gu, K. Flippo, and D. Umstadter, Phys. Rev. Lett. **84**, 4108 (2000).
7. E. L. Clark, K. Krushelnick, M. Zepf et al., Phys. Rev. Lett. **85**,1654 (2000).
8. J. Denavit, Phys. Rev. Lett. **69**, 3052 (1992).
9. L. O. Silva, M. Marti, J. R. Davies et al., Phys. Rev. Lett. **92**, 015002 (2004).
10. M. S. Wei, S. P. D. Mangles, Z. Najmudin et al., Phys. Rev. Lett. **93**, 155003 (2004).
11. A. Zhidkov, M. Uesaka, A. Sasaki, and H. Daido, Phys. Rev. Lett. **89**, 215002 (2002).
12. O. Shorokhov and A. Pukhov, Laser Part. Beams **22**, 175 (2004).
13. S. Wilks, A. B. Langdon, T. E. Cowan et al., Phys. Plasmas **8**, 542 (2001).
14. A. Puchov, Phys. Rev. Lett. **86**, 3562 (2001).
15. M. Zepf, E. L. Clark, F. N. Beg et al., Phys. Rev. Lett. **90**, 064802 (2003).
16. S. Karsch, S. Düsterer, H. Schwoerer et al., Phys. Rev. Lett. **91**, 015001 (2003).
17. M. Kaluza, J. Schreiber, M. I. K. Santala et al., Phys. Rev. Lett. **93**, 045003 (2004).
18. S. C. Wilks, W. L. Kruer, M. Tabak, and A. B. Langdon, Phys. Rev. Lett. **69**, 1383 (1992).
19. E. Lefebvre and G. Bonnaud, Phys. Rev. E **55**, 1011 (1997).
20. W. L. Kruer and K. Estabrook, Phys. Fluids **24**, 430 (1985).
21. T. Tajima and J. M. Dawson, Phys. Rev. Lett. **43**, 267 (1979).
22. A. Pukhov, Z.-M. Sheng and J. Meyer-ter-Vehn, Phys. Plasmas **6**, 2847 (1999).
23. J. Stein, E. Fill, G. Pretzler, and K. Witte, Laser Part. Beams **22**, 315 (2004).
24. J. Fuchs, Y. Sentoku, S. Karsch et al., Phys. Rev. Lett. **94**, 045004 (2005).
25. M. P. Kalachnikov, M. P. Karpov, V. Schönnagel, and W. Sandner, et al., Laser Physics **12**, 368 (2002).
26. S. Ter-Avetisyan, M. Schnürer, S. Busch et al., Phys. Rev. Lett. **93**, 155006 (2004).
27. S. Ter-Avetisyan, M. Schnürer, and P. V. Nickles, J. Phys. D: Appl. Phys. **38**, 863 (2005).
28. J. Schreiber, S. Ter-Avetisyan, E. Risse et al., Phys. Plasmas (submitted).
29. M. V. Ammosov, N. B. Delone, and V. P. Krainov, ZhETF **91**, 2008 (1986) [Sov. Phys. JETF **64**, 1191 (1986)].